A STUDY OF SPACR GHOST DYNAMICS APPLIED TO RNAV ROUTES IN THE TERMINAL AREA

Arthur P. Smith and Thomas A. Becher
The MITRE Corporation, McLean, Virginia

Abstract

Current terminal operations are changing as more terminal Area Navigation (RNAV) routes are defined that aircraft are expected to fly. Previously, arriving aircraft filing a Standard Terminal Arrival Route (STAR) were given vectors to guide them to the runway when the aircraft transitions from the STAR and enters the terminal area. There are, however, efforts underway to extend these STARs as routes in the terminal area that overlay the current traffic patterns resulting from the vectors that controllers give to the aircraft. To achieve the expected benefits from these terminal routes, the controllers will need automation support to assist them in managing the traffic where the routes merge.

Many automation aids could be envisioned to assist the controllers. One particular suite of tools called Spacing of Performance-based Arrivals on Converging Routes (SPACR) has been discussed previously. In that tool set there is a controller decision aide called Converging Route Display Aid (CRDA). The genesis of this decision aid was the Converging Runway Display Aid which is currently embedded in all the Automated Radar Terminal System (ARTS) and Standard Terminal Automation Replacement System (STARS) computers in the United States. In its current form CRDA is a useful decision support tool as part of SPACR to address uncoordinated terminal merges. However, because of the potential geometries of the RNAV routes in the terminal area, CRDA could be more useful with expanded functionality.

In the past certain extensions to CRDA have been investigated. Many of these extensions have resulted in unstable or undesirable dynamics of the "ghost" targets such as jumping and hesitation. This paper will define alternative functional extensions to target aircraft detection and ghost projection that will be useful for RNAV routes and provide the results of analyses performed to determine the effectiveness of such extensions. In particular we will show that if the aircraft conform closely to the RNAV route the "ghost" targets will behave in a manner that should be acceptable to controllers, based upon past controller feedback. We will also show under what conditions the dynamics of the "ghost" targets behave badly.

Background

To maintain the benefits of a route structure in the terminal area it is necessary for the aircraft to remain on the routes for as long as possible. The natural inclination for controllers is to provide vectors to the aircraft as a control strategy when the aircraft enter the terminal area on a standard arrival route (STAR). As this would take the aircraft off the route, other strategies need to be developed to insure that the aircraft fly along the assigned route. A suite of tools called Spacing of Performance-based Arrivals on Converging Routes (SPACR) has been proposed [1] to support strategies of keeping aircraft on routes in the terminal area.

One of the tools in that suite is Converging Route (Runway) Display Aid (CRDA). Historically, this tool has been used to synchronize aircraft on approach to two runways. It was introduced into the National Airspace System (NAS) in 1991 and currently is implemented in all NAS terminal automation systems.

The concept of CRDA is very simple in that it projects a ghost target based on the position of an aircraft target [2]. The ghost target represents where the aircraft would be on the other approach. The controller then spaces his aircraft from the ghost to achieve the desired synchronization of the aircraft. There are also variations of this concept where the ghost is placed such that the controller places his aircraft on top of the ghost to achieve the synchronization.

Over the years, several facilities have implemented procedures using CRDA. In the mid-1990s the New York Terminal Radar Approach

Control (TRACON) experimented with using CRDA to synchronize aircraft on a curved approach with aircraft on a straight-in approach at Newark. A new ghosting algorithm was designed for this operation and was called Adaptive Path Ghosting (APG) [3]. This form of ghosting was never used at the New York TRACON because the algorithm was too sensitive to the amount of vectoring that was performed near to the airport.

Problem Description

The problem with the current implementation of CRDA, including APG, is that it is not able, in general, to generate ghost targets on multi-segmented routes in the terminal area that are acceptable to controllers. In addition, the qualification region for each segment is constrained to be a trapezoidal shape with the parallel sides perpendicular to the route segment. This causes gaps and overlaps between the qualification regions of the two adjoining route segments. In the current implementation, if the aircraft is within a gap or an overlap, no ghost target is produced.

To generate ghosts that are acceptable to controllers, the ghosts need to have dynamics similar to the dynamics of a real aircraft. This means that from radar scan to radar scan the ghost targets must produce a track that is continuous and the distances between the successive ghost targets are representative of the speed of the aircraft creating the ghost.

From laboratory experience and also in actual operational environments, if the ghost of an aircraft does not perform in a predictable manner related to the track of the aircraft creating the ghost, the controllers will not be able to use the ghost target.

The following section proposes two designs for generating ghosts from aircraft flying a segmented path in the terminal area. The merits of both designs will be discussed and compared.

Proposed Solutions

The basic design principle is that the ghost should depend only on the position of one aircraft. The design of APG used the position of the aircraft plus the positions of all the aircraft in front of it to determine the placement of the ghosts. This adds complexity such as determining the sequence of the aircraft. It also introduces other effects that cause the ghosts to behave in unexpected ways.

The other design principle is that the ghost should appear on the second route, regardless of whether that route is a series of connected linear segments or not. This argues for the position of the aircraft to be mapped into a distance which can then be measured along the second route from a predetermined reference point.

To investigate both designs a set of tracks that are representative of a flow of traffic was considered. The four tracks shown in Figure 1 were actual Automated Radar Terminal System (ARTS) tracks flown by four consecutive flights in the Philadelphia terminal airspace. These aircraft were vectored to the downwind leg of the approach. Since the tracks of most of the flights during this time period followed generally the same pattern, a route was hypothesized. This route is also shown in Figure 1.

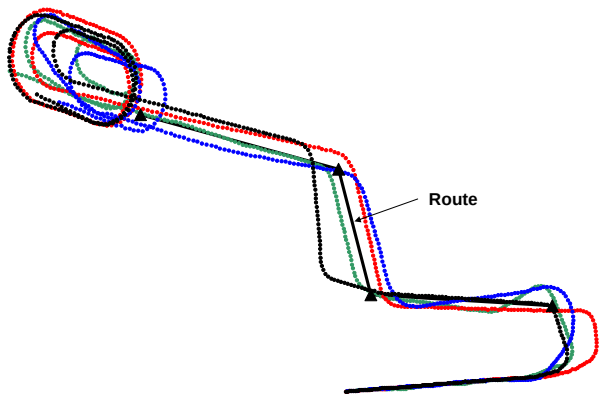

Figure 1. Vectored Tracks to Test Ghost Designs

For an RNAV/RNP route the tracks in Figure 1 could be considered to be a “worst case”. More likely the tracks would look like those in Figure 2. This could be considered to be the “best case”.

Design 1

The first design measures the aircraft’s distance from the target reference point (in this case, the waypoint on the right end of the route in Figures 1 and 2) by measuring the distance from the aircraft to the next waypoint and then adding the

sum of the distances between the succeeding waypoints.

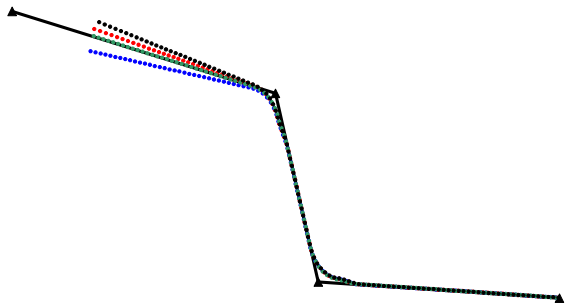

Figure 2. RNAV Tracks to Test Ghost Dynamics

There are two considerations needed to define this process. One is to identify which radar returns will be eligible to create a ghost and the other is to determine which waypoint is the next waypoint.

The qualification of the radar returns is accomplished by enclosing the route segments of interest with a closed polygonal region. Such a qualification region is shown in Figure 3. This region will prevent radar returns on the base leg and the final approach from creating ghosts. This region could also have other attributes such as a ceiling or floor or heading tolerances to differentiate aircraft flying the route from other aircraft that might be flying through the airspace.

In this first design, determining which waypoint is the next waypoint is accomplished by a set of parabolas. The motivation for using parabolas is as follows: in the case where an aircraft is off the route (see the turning late aircraft in Figure 3), the closer the aircraft approaches the waypoint, the more likely it will be that the distance between the aircraft and the waypoint will actually starting increasing. This would cause a ghost to appear to slow down. Therefore, it would be beneficial for the aircraft to be associated with the next waypoint as early as possible. It turns out that testing whether the aircraft's radar return is on one side of a parabola or the other is a fairly easy test. The parabola also has the feature of allowing the association with the next waypoint earlier for those returns that are farther from the route. The parabolas that were chosen for this analysis are shown in Figure 3. In particular the perpendicular distance between the focus and the directrix of these parabolas are 4 nm. In this figure the parabolas are labeled as the segment boundaries. The positions where the tracks cross the segment boundaries are called the segment transitions.

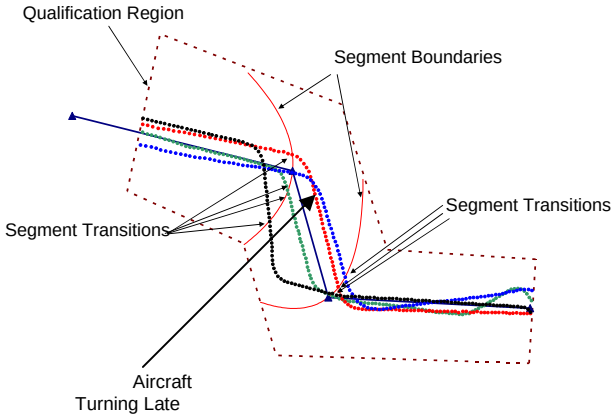

Figure 3. Qualification and Segment Definitions for Design 1

To observe how the ghosts produced by the first design behave, each of the four tracks was simulated and the distances to the target reference point were measured for each radar update. Next, the speeds of the ghosts were ascertained by dividing the change in the ghost distance by the time interval of the radar scans. The ghost speeds were then compared to the speed of the aircraft computed in the same manner.

The results of the comparison of the ghost speed with the aircraft speed for the vectored tracks are shown in Figure 4.

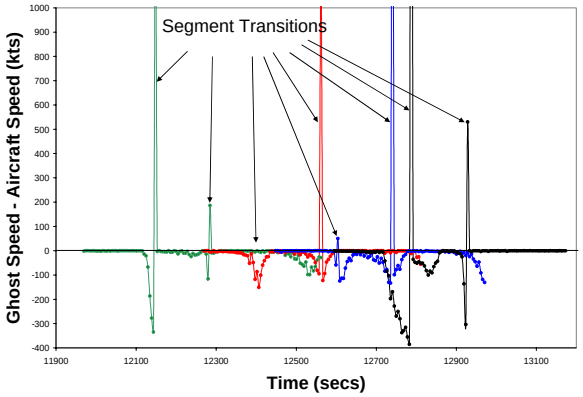

Figure 4. Ghost Speeds Compared to Aircraft Speeds – Design 1, Vectored Tracks

The colors of the plots in Figure 4 correspond to the colors of the tracks in Figures 1 and 3. The first track (green) flies down the first segment of the route and then "cuts the corner" before getting to the second waypoint. This is reflected in the speed plot as the ghost speed becoming slower than the aircraft speed (i.e., a negative speed difference in Figure 4). As the first aircraft flies across the segment boundary the speed of the ghost increases dramatically for one scan. This will be perceived by the controller as the ghost "jumping". As the first aircraft reaches the third waypoint, the ghost slows slightly with respect the aircraft speed and then jumps as it transitions to the next segment. At the end of the track the first aircraft is vectored north of the route which causes the ghost to slow down relative to the aircraft speed.

Each of the other tracks exhibit similar behavior. The fourth aircraft (black) appears to be worst case among the four. Notice in Figure 3 that the black track is vectored south before reaching the second waypoint. Since the aircraft is not moving towards the second waypoint, the ghost will slow down for several radar scans before the aircraft flies over the segment boundary and is associated with the third waypoint. A single scan jump might be tolerated by the controllers if it is predictable. However, several consecutive scans at a significantly slower speed will be noticed by the controllers.

If the RNAV tracks are processed the same way as the vectored tracks were, then the resulting ghost speeds relative to the aircraft speeds are shown in Figure 5.

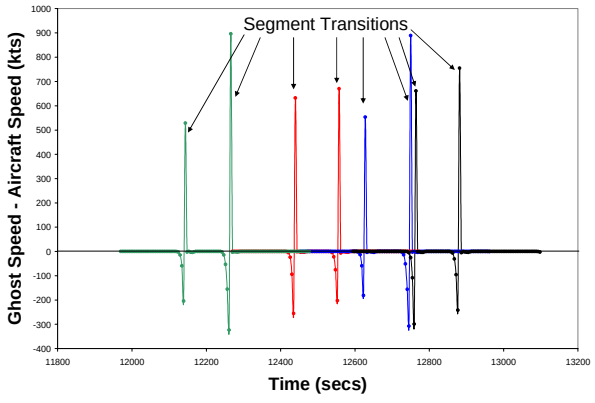

Figure 5. Ghost Speeds Compared to Aircraft Speeds – Design 1, RNAV Tracks

Since the aircraft on RNAV tracks do not fly exactly over each waypoint, there will still be a jump as the aircraft transitions from one segment to another. However, the jumps are limited to just a few scans. In addition, since the tracks will be basically the same, the jumps will be very predictable.

Design 2

This method mitigates the issues of ghost aircraft jumping and stalling by providing a projection that accounts for aircraft making turns. In this design, there is a reference path and reference point and an image path and image point. The reference path and image path are both piecewise linear to match the lateral path associated with an arrival procedure. The reference point and image point are arbitrarily placed points a distance from the end of each path. Figure 6 provides an example of a reference path and an image path where the reference point and image point are both located at the end of each path. The notion of introducing paths reflects the trend for many terminal facilities to introduce RNAV arrival routes. These routes may be based upon replacing vectored paths with an RNAV route or creating a new arrival path for a new runway or optimization of existing arrival flows. For a four-corner-post operation, there are arrival routes that bring aircraft from the four-corner-posts and deliver them to the runways. Depending upon the operation, e.g., landing aircraft from the North, South, East, or West, there will be a pair of routes that are shorter and more direct to the runways and a pair that are longer. The longer routes bring aircraft on a downwind, base, and turn to final. From the entry fixes, there may be some pre-final merges and ultimately the merge of two or more major streams on final. The example in Figure 6 represents an arrival path delivering aircraft onto a downwind and the other path representing aircraft arriving directly to final approach. It has already been demonstrated that classic ghosting is a tool for helping to manage merges. Classic ghosting suffers from jumping, stalling, and ghost aircraft appearing and disappearing when ghosting regions partially overlap. This technique eliminates those issues. This technique also preserves the ground speed of aircraft when projecting from one straight segment onto another straight segment. Some variation is

introduced to the speed when projecting from a turn to a straight segment or a turn segment.

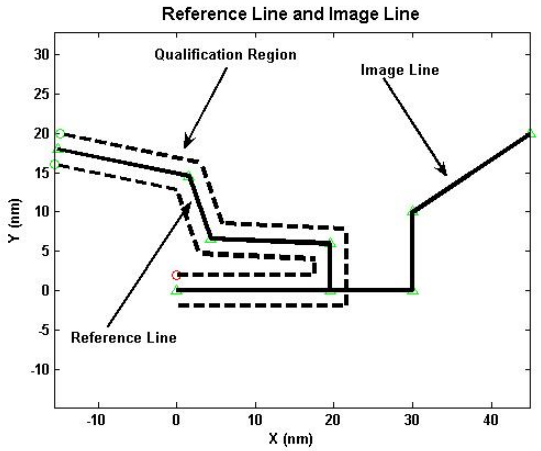

Figure 6. Reference Line and Image Line

Derivation of Projection Methods

Given a piece-wise linear reference line defined by a series of waypoints (which can be converted to a series of (x, y) points), the qualifying region is defined by the region bounded by a set of parallel lines a distance D1 and D2 on either side of the reference line and the lines perpendicular to the reference path at the first and last point. The qualifying region is partitioned into straight rectangular regions and turn regions. This definition of a qualifying region eliminates the problem of piecing together trapezoidal regions of classic ghosting which may overlap (creating multiple ghosts) or have gaps (causing ghost aircraft to disappear and reappear). The qualifying regions could be generalized to be a contiguous set of quadrilateral regions with non-overlapping turn regions. Generalizing the qualification regions in this manner will make it easier to adapt the application to regions that have non-uniform traffic dispersion. Without loss of generality, all analysis done will be done assuming parallel lines defining the qualifying regions and non-overlapping turn regions.

To define the straight and turn qualifying regions, at each turn, the slope of the line that bisects the course change angle for each turn is constructed. Refer to Figure 7.

The slope of the bisector line is determined by constructing two lines the same distance on the either side of the waypoint defining the turn by the lines perpendicular to the inbound segment and outbound segment. The intersection of these two lines lies on the bisector and is denoted by (x_c, y_c).

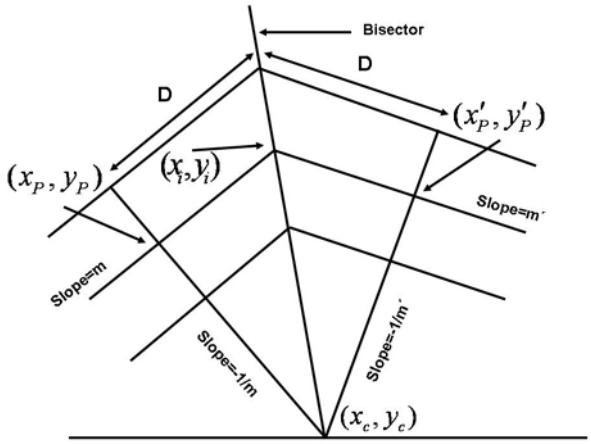

Figure 7. Turn Qualifying Regions Construction

Using this intersection point and the turn point (x_i, y_i), the slope of the bisector line is determined. Once the bisector line slope is determined, the intersection points of the parallel lines are determined. The equation of the inboard segment is given by $y = m(x - x_i) + y_i$ and the line perpendicular to the inbound segment is given by $y = -1/m(x - x_c) + y_c$. The intersection point with the inbound segment (x_P, y_P) is given by:

$$x_P = \frac{m^2 x_i + x_c + m(y_c - y_i)}{1 + m^2}$$

$$y_P = \frac{m^2 y_c + y_i + m(x_c - x_i)}{1 + m^2}$$

The beginning and ending straight segments are defined by lines which are perpendicular to the first and last segment that go through the first and last point respectively that define these segments and the perpendicular lines associated with the adjacent turn as explained below.

The next step needed to define the turn regions is to determine the turn center for each turn which is defined by determining the point that is a distance L from the turn point along the bisector line. See Figure 8. There are two possible solutions for a point that is a distance L from a given point on a line. The boundary line to use is determined by whether the turn is a right-handed turn or a left-handed turn along with the proper sign to select

the proper solution. The handedness of the turn is determined by computing the cross product of vectors that point from the start point of the segment to the end point for the two segments defining the turn.

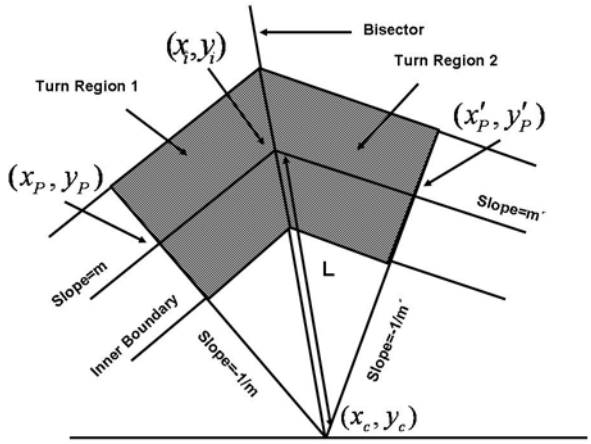

Figure 8. Determination of Point (x_c , y_c)

After the center point is determined, then the start and end of the turn is defined by a line perpendicular to the slope of the incoming course line and outgoing course line that intersect at the center point. A turn region is defined by two regions: the first region is bounded by the line perpendicular to the inbound course and the bisector and bounded by the parallel boundary lines to the inbound course, the second region is bounded by the bisector and the line perpendicular to the outbound course and bounded by the parallel boundary lines to the outbound course. A different value for L can be chosen for each turn. The value of L can be determined statistically by analyzing a collection of recorded track data over periods of time when the arrival paths are heavily used. L could also be determined by using the typical ground speed of aircraft when making the turn and assuming a nominal bank angle in the range of 18 to 23 degrees and using the formula:

$$R = v_g^2 / (g \tan \phi)$$

where g is the acceleration of gravity and ϕ is the bank angle. Figure 9 illustrates the turn projection algorithm.

After the turn regions are defined, the qualification region along the reference path can now be partitioned into a series of rectangular regions and turn regions. For aircraft in a rectangular qualification zone (could be a quadrilateral region), the aircraft position is projected onto the reference

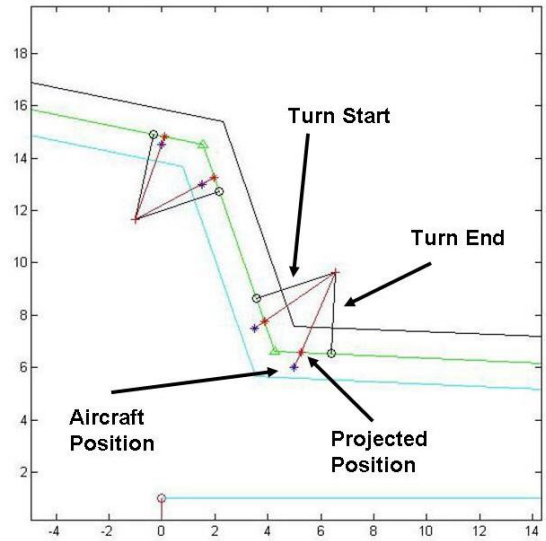

Figure 9. The Turn Project Algorithm

line segment by constructing a line perpendicular to the reference line segment and going through the aircraft position. The offset distance of the aircraft is recorded along with the distance of the aircraft projection point from the reference line point (essentially distance remaining). If the aircraft position enters a turn qualification region, the aircraft projection point is determined by computing the intersection of the line defined by the aircraft and going through the turn center point with the reference line segment (projecting along a radial rather than perpendicular). The offset distance from the reference line along the radial is recorded as well as the distance remaining for the projection point along the reference path. This information is used for determining the ghost position along the image reference path.

The ghost aircraft position on the image line is determined by computing the distance along the image path from the image point and then offsetting that point either along a perpendicular line or radial based upon whether the point is on a straight segment or turn segment. The image path is partitioned into a series of straight and turn segments. If the projected point falls into a rectangular region, then the ghost position is created by projecting the lateral offset distance, in either

direction, perpendicular to the line segment. If the projected point falls into a turn region, then the projected point from the rectangular reference region is projected along a radial that goes through the turn center. The lateral distance along the radial is computed and distance from the projected point to the reference point is calculated. This distance is used to obtain the point along the image line path, as before.

Figure 10 illustrates application of this algorithm to one of the tracks. Note that there are no gaps or jumps in either path. The two turns are visible on the image path. The first turn is on a straight segment on image path and the second turn is mapped to a turn on the image path. The ghost position moves out laterally to a maximum distance (corresponding to the midpoint of the turn) and then moves the same distance closer.

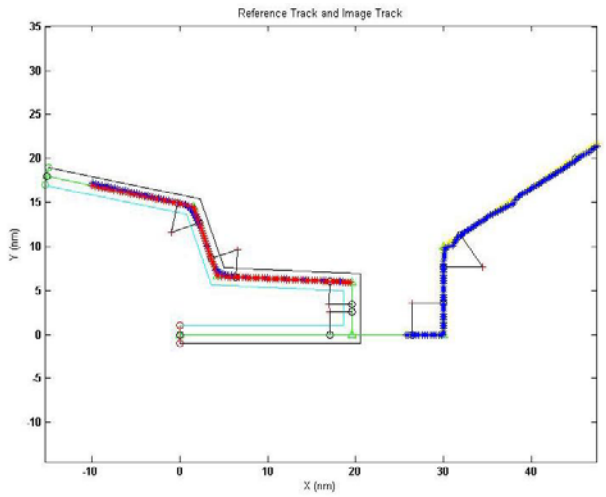

Figure 10. Reference Track and Image Track

The projection of the aircraft position from a reference path rectangular region to straight segment on the image path preserves the ground speed of the aircraft. The proof of this is provided in Appendix A. The projection of aircraft position in a turn on the reference path onto a straight segment in the image path does not preserve the aircraft speed. It can be shown (see Appendix A) that the speed of the projection points on a reference path turn for an aircraft following a turn at constant speed is given by

$$v_I = \begin{cases} v_g(1+\tan^2(\omega(t-t_o)) & t_o \le t \le t_o + \dfrac{\theta}{2\omega} \\ v_g(1+\tan^2(\theta-\omega(t-t_o)) & t_o + \dfrac{\theta}{2\omega} \le t \le t_o + \dfrac{\theta}{\omega} \end{cases}$$

where v_g is the aircraft ground speed, θ is the course change angle for the turn, and $\omega = v_g / R$ is the angular turn rate. This result shows that the growth rate depends only on the magnitude of the course change angle and the turn rate. This shows that the speed along the reference path increases approximately quadratically to its maximum value at the midpoint of the turn and then decreases quadratically. When projecting onto a straight image segment, this is the best behavior than can be expected for the ghost speed. Figure 11 illustrates that the aircraft speed is preserved on straight segments and that there is an increase and then decrease in the ghost speed through a turn.

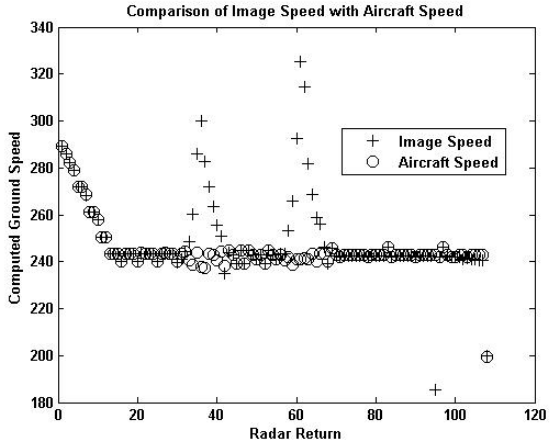

Figure 11. Comparison of Image Speed with the Aircraft Speed

Figure 12 shows an example of a recorded track that extends all the way to the runway. The qualification region also extends to the runway and the image path represents a typical path for arrivals from a northeast TRACON entry fix.

One of the issues investigated by introducing alternate ghosting methods is the appearance of the ghost on the image path. This example illustrates the difference between only displaying the image points on the image path versus including the lateral offset associated with the aircraft relative to the

reference path. It will be interesting to obtain controller feedback on the behavior of the ghost. The only unphysical behavior with this technique is the ghost speed. The only way to eliminate the unphysical behavior of the ghost speed is to use

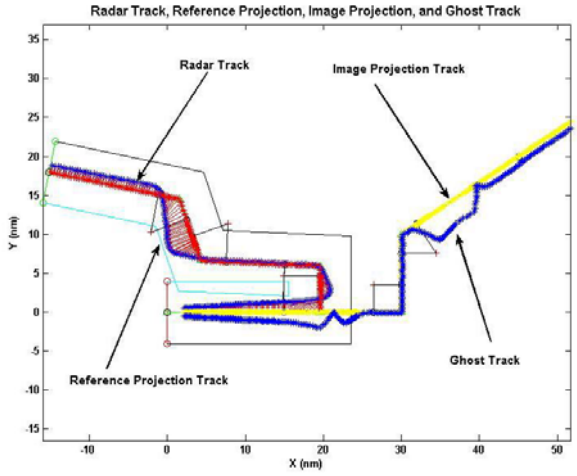

Figure 12. Radar Track, Reference Projections, Image Projection and Ghost Track

circular arcs as part of the image path and reference path. The problem with introducing a circular arc is that it will not match for all the aircraft executing turns. The projection speed on the reference line will be rescaled by the ratio of the actual turn radius of the aircraft with the turn radius of the reference path. This will be minimized for procedures that use radius-to-fix (RF) legs. For these legs, all aircraft will execute the same circular ground track which will eliminate the unphysical speed behavior. Such approach procedures are currently under implementation at several sites throughout the U.S. The procedures are called Special Aircraft and Aircrew Authorization Required (SAAAR) procedures that take advantage of the Required Navigation Performance (RNP) capability available today. The SAAAR procedures use the RF leg for curved approaches. When the procedure is published, the turn radius and center for the RF is available as part of the procedure. This information could then be made available to the ground automation so that the same turn radius is used in the projection algorithm. With this information, the unphysical speed behavior of the ghosts would be eliminated.

It is worth noting that the most complex mathematical operation used in this algorithm for defining the qualification regions and the projections is a square root. All the other operations are simple algebraic manipulations that do not require the evaluation of trigonometric functions. For the ARTS IIIA and IIIE systems, there are limitations on the mathematical functions that are supported. These algorithms are not restricted by such limitations.

Conclusions/Next Steps

Both of the designs presented had as their goal to eliminate or mitigate undesirable behavior that in the current operational implementation of ghosting in the ARTS and STARs terminal systems. Since ghost qualification regions must be trapezoids with reference lines perpendicular to the parallel sides, successive qualification regions following a segmented path will result in the qualification regions having gaps or overlaps. Under these conditions, the ghost aircraft will disappear when the parent aircraft is in the gap or overlapping region and then reappear. Ghost aircraft will also exhibit unphysical behavior such as stalling, jumping, and going in reverse under some circumstances.

Two methods were analyzed for addressing these issues. Both designs applied the rule that the ghost position depends only on the position of one aircraft and that the ghost appears on the image path where the image path can also be a segmented route. Both designs employed contiguous quadrilateral qualification regions that could be augmented with additional filters such as altitude, heading, speed, and scratch pad entry. The first design uses parabolas to define segment transitions and to assign along path distance to an aircraft. This along path distance is then projected on the image path to obtain the location of the ghost. Design 1 did not compute a lateral offset for the aircraft. Design 2 partitioned the qualification regions along the reference path into rectangular regions and turns. For aircraft in the rectangular regions, the along path distance was computed along with a perpendicular offset. For aircraft in turn regions, the along path distance and lateral offset was determined by a radial that intersected the reference path. The ghost position was then determined by projecting back along the image path (also partitioned into straight and turn segments)

and offsetting a perpendicular amount if on a straight segment and along a radial if on a turn.

Both methods still introduce some unphysical behavior for the ghost speed. Design 1 experienced speed spikes when transitioning across segment boundaries. Design 2 experienced an oscillation in the ghost speed for the turn segments where the ghost speed equals or exceeds the aircraft speed. The magnitude of the oscillation is determined by the turn rate and the turn radius. Since Design 2 also computed the lateral offset for the ghost, when aircraft turned, the ghost would veer away from the image path and then return.

Both designs eliminated disappearing and then reappearing ghosts. Design 2 also eliminated stalling and jumping but the ghost may leave the image route when the airline enters a turn. Design 1 still has the potential for stalling and jumping but the length of time that the aircraft slows down and speeds up can be quite short. For both of these designs, controller feedback will be required to determine if this speed behavior is noticeable and whether the ghost position with lateral offset is desirable rather than just showing the projected position on the path.

References

[1] Becher, Thomas A., David R. Barker, Arthur P. Smith, 2004, *Methods for Maintaining Benefits for Merging Aircraft on Terminal RNAV Routes*, 23rd DASC, Salt Lake City, UT.

[2] Mundra, Anand D., 1989, *A New Automation Aid to Air Traffic Controllers for Improving Airport Capacity*, MP-89W00034, The MITRE Corporation, McLean, VA.

[3] Smith, Arthur P., 1996, *Specification for the Adaptive Path Ghosting Function of the Controller Automated Spacing Aid (CASA)*, MTR-96W00011-3, The MITRE Corporation, McLean, VA.

Disclaimer

The contents of this material reflect the views of the authors. Neither the Federal Aviation Administration nor the Department of Transportation makes any warranty, guarantee, or promise, either expressed or implied, concerning the content or accuracy of the views expressed herein.

Email Addresses

Arthur P. Smith apsmith@mitre.org

Thomas A. Becher tbecher@mitre.org

24th Digital Avionics Systems Conference
October 30, 2005

Appendix I

Modulation of Ghost Speed on Turn

Consider a turn as depicted in Figure A-1.

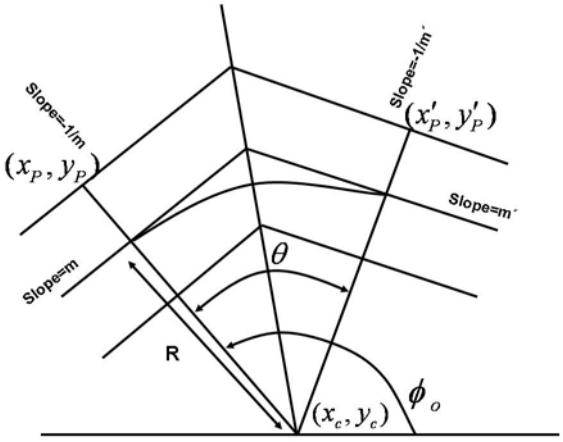

Figure I-1. Turn Geometry

Assume that the aircraft is flying a circular arc, and then the position of the aircraft relative to the turn center (x_c, y_c) is given by:

$$x_{ac} = -R\cos(\phi_o - \omega(t - t_o))$$
$$y_{ac} = R\sin(\phi_o - \omega(t - t_o)) \quad (1)$$

where ϕ_o is the initial phase of the turn, R is the turn radius, ω is the angular turn rate given by the ground speed divided by the turn radius, and t is the time. At $t = t_o$, $\tan(\phi_o) = y_P / x_P = -1/m$ where m is the slope of the inbound segment and (x_c, y_c) was chosen to be $(0,0)$ for convenience. The equation of the radial defined by the aircraft position is given by:

$$y = M(x - x_c) + y_c = Mx \tag{2}$$

and

$$M = (y_{ac} - y_c)/(x_{ac} - x_c) = y_{ac} / x_{ac} \tag{3}$$

Therefore,

$$M = \tan(\phi_o - \omega(t - t_o)) \tag{4}$$

and

$$\dot{M} = (-v_g / R)\sec^2(\phi_o - \omega(t - t_o)) \tag{5}$$

The equation of the inbound course segment is given by:

$$y = m(x - x_P) + y_P \tag{6}$$

The intersection point of the radial with the inbound course segment is obtained by solving equations (2) and (6) simultaneously with the result:

$$x_I = \frac{Mx_c - mx_P + y_P - y_c}{M - m}$$
$$y_I = \frac{My_P - my_c + mM(x_c - x_P)}{M - m} \tag{7}$$

For $(x_c, y_c) = (0,0)$ equation (7) becomes:

$$x_I = \frac{y_P - mx_P}{M - m}$$
$$y_I = \frac{M(y_P - mx_P)}{M - m} \tag{8}$$

Taking the time derivatives of equation (8), we obtain:

$$\dot{x}_I = -\frac{\dot{M}(y_P - mx_P)}{(M - m)^2}$$
$$\dot{y}_I = -\frac{m\dot{M}(y_P - mx_P)}{(M - m)^2} \tag{9}$$

The speed of the projection point is given by:

$$v_I = \frac{\dot{M}(y_P - mx_P)\sqrt{1 + m^2}}{(M - m)^2}$$
$$= v_g \frac{(1 + m^2)\sec^2(\phi_o - \omega(t - t_o))}{\left[\tan(\phi_o - \omega(t - t_o)) - m\right]^2} \tag{10}$$

where $y_P / R = 1/\sqrt{1 + m^2}$ was used along with equations (4) and (5). Using the trigonometric identity:

$$\tan(\phi_o - \omega(t - t_o)) = \frac{\tan\phi_o - \tan\omega(t - t_o)}{1 + \tan\phi_o \tan\omega(t - t_o)}$$
$$= \frac{1 + m\tan\omega(t - t_o)}{-m + \tan\omega(t - t_o)} \tag{11}$$

and

$$\tan(\phi_o - \omega(t - t_o)) - m = \frac{1 + m^2}{-m + \tan\omega(t - t_o)} \tag{12}$$

equation (10) simplifies to:

$v_I = v_g(1 + \tan^2\omega(t - t_o))$ valid for $0 \le t - t_o \le \theta/(2\omega)$. For $\theta/(2\omega) \le t - t_o \le \theta/\omega$,

$$x_{ac} = -R\cos(\phi_o - \theta - \omega(t - t_o))$$
$$y_{ac} = R\sin(\phi_o - \theta - \omega(t - t_o)) \tag{13}$$

Repeating a similar reasoning using:

$$x'_P = R\cos(\phi_o - \theta)$$
$$y'_P = R\sin(\phi_o - \theta) \tag{14}$$

and

$y'_P / x'_P = \tan(\phi_o - \theta) = -1/m'$, we can derive:

$$v_I = v_g\left(1 + \tan^2\left(\theta - \omega(t - t_o)\right)\right) \tag{15}$$

Preservation of Aircraft Speed When Projecting From Rectangular Region to Straight Segment

The projection of the aircraft position in a rectangular qualification region to a straight segment consists of the following operations: (1) compute the perpendicular offset and the intersection point on the reference line, (2) rotate the line to a new orientation (translate the image line segment so that it shares a common origin with the reference line segment since translation by a constant offset does not impact speed), and (3) compute the perpendicular offset of the ghost relative to the image line.

Let d denote the perpendicular offset distance of the aircraft from the reference line segment and let (x_{ac}, y_{ac}) denote the aircraft position. The intersection point of the line which is perpendicular to the reference line and goes through the aircraft position is given by:

$$x' = x_{ac} + md / \sqrt{1+m^2}$$
$$y' = y_{ac} + d / \sqrt{1+m^2} \tag{16}$$

where $m = \tan\phi$ is the slope of the reference line segment. Taking the time derivative, we see that:

$$v_g = \sqrt{\dot{x}_{ac}^2 + \dot{y}_{ac}^2} = \sqrt{(\dot{x}'_{ac})^2 + (\dot{y}'_{ac})^2} \tag{17}$$

Rotating (x', y') to a new point (x'', y'') on a straight line with slope $m' = \tan\theta$,

$$x'' = x'\cos\theta + y'\sin\theta$$
$$y'' = x'\sin\theta - y'\cos\theta \tag{18}$$

and

$$x_G = x'\cos\theta + y'\sin\theta + d / \sqrt{1+m'^2}$$
$$y_G = x'\sin\theta - y'\cos\theta + dm' / \sqrt{1+m'^2} \tag{19}$$

Taking the time derivative, we see that:

$\sqrt{\dot{x}_{ac}^2 + \dot{y}_{ac}^2} = \sqrt{(\dot{x}_G)^2 + (\dot{y}_G)^2}$. Using equation (19), the ghost position can be expressed in terms of the slopes of the two lines and is given by:

$$x_G = \left(x_{ac} + \frac{md}{\sqrt{1+m^2}}\right)\frac{1}{\sqrt{1+m'^2}} + \left(y_{ac} + \frac{d}{\sqrt{1+m^2}}\right)\frac{m'}{\sqrt{1+m'^2}} + \frac{d}{\sqrt{1+m'^2}}$$
$$y_G = \left(x_{ac} + \frac{md}{\sqrt{1+m^2}}\right)\frac{m'}{\sqrt{1+m'^2}} - \left(y_{ac} + \frac{d}{\sqrt{1+m^2}}\right)\frac{1}{\sqrt{1+m'^2}} + \frac{dm'}{\sqrt{1+m'^2}} \tag{20}$$